Tabelle 4. $Co^{II}$- *und* $Co^{III}$-*Sauerstoff-Abstände* (Å), *berechnet mit einem mittleren Sauerstoffradius von* 1,37 Å *aus Ionenradien nach Shannon* (1976) *bzw. beobachtet* (*Mittelwerte*)

| | berechnet | | beobachtet |
|---|---|---|---|
| | 'high spin' | 'low spin' | |
| $Co^{II}$, tetraedrisch | 1,95 | — | 1,959 |
| $Co^{II}$, oktaedrisch | 2,115 | 2,02 | 2,111 |
| $Co^{III}$, oktaedrisch | 1,98 | 1,915 | 1,905 |

hervorgehoben (Trömel, 1983*a*). Man kann annehmen, dass in den Fällen, in denen starke Abweichungen auftreten, neben den Bindungsstärken noch andere Faktoren die Bindungslängen beeinflussen. Im Falle der oktaedrischen Koordination von $Co^{III}$ scheinen die Bindungen aufgrund von 'low-spin'-Konfiguration am Kobalt verkürzt zu sein. Hierfür spricht der Vergleich der beobachteten Bindungslängen mit denen, die sich aus Ionenradien nach Shannon (1976) mit einem Sauerstoffradius von 1,37 Å berechnen, wie er sich auch sonst zur Verknüpfung von Bindungslängen–Bindungsstärken-Beziehungen mit Ionenradien eignet (Trömel, 1983*a*). Die Gegenüberstellung der berechneten und beobachteten Abstände (Tabelle 4) zeigt ausgesprochen gute Übereinstimmung für die $Co^{II}$-'high-spin'- und $Co^{III}$-'low-spin'-Konfigurationen. $Co^{II}$, nicht aber $Co^{III}$, scheint sich in dieser Hinsicht den Elementen Titan bis Eisen anzuschliessen, bei denen die berechneten Bindungslängen, soweit unterscheidbar, durchweg den 'high-spin'-Ionenradien bzw. den daraus berechneten Abständen entsprechen. Schon für $Co^{IV}$ in tetraedrischer Koordination kommt eine solche Interpretation aber nicht mehr in Betracht, da hier Abweichungen zu höheren und niedrigeren Werten auftreten. Auch die Sonderstellung der $Cu^{I}$-Sauerstoff-Koordination kann auf diese Art nicht verständlich gemacht werden. Sie steht wohl eher in Zusammenhang mit der abgeschlossenen *d*-Schale des einwertigen Kupfers.

Ich danke dem Hochschulrechenzentrum der Universität Frankfurt für Rechenzeit an der DEC 1091, mit der die umfangreicheren Rechnungen ausgeführt wurden.

**Literatur**


ALCOCK, N. W. (1972). *Adv. Inorg. Chem. Radiochem.* **15**, 1–58.

ARENDALE, W. F. & FLETCHER, W. H. (1953). *J. Chem. Phys.* **21**, 1898.

BARBIER, P., MAIRESSE, G. & WIGNACOURT, J. P. (1976). *Cryst. Struct. Commun.* **5**, 633–637.

BROWN, I. D. & WU, K. K. (1976). *Acta Cryst.* B**32**, 1957–1959.

DOHLEN, W. C. VAN & CARPENTER, G. B. (1955). *Acta Cryst.* **8**, 646–651.

DONNAY, G. & ALLMANN, R. (1970). *Am. Mineral.* **55**, 1003–1015.

HAGEN, K. & HEDBERG, K. (1973*a*). *J. Am. Chem. Soc.* **95**, 1003–1009.

HAGEN, K. & HEDBERG, K. (1973*b*). *J. Am. Chem. Soc.* **95**, 4796–4800.

HARMONY, M. D., LAURIE, V. W., KUCZKOWSKI, R. L., SCHWENDEMAN, R. H., RAMSAY, D. A., LOVAS, F. J., LAFFERTY, W. J. & MAKI, A. G. (1979). *J. Phys. Chem. Ref. Data*, **8**, 619–721.

*International Tables for X-ray Crystallography* (1968). Bd. III. Birmingham: Kynoch Press.

LIVINGSTON, R. L. & RAO, C. N. R. (1959). *J. Am. Chem. Soc.* **81**, 285–287.

POLL, W. (1983). Dissertation, Düsseldorf.

SHANNON, R. D. (1976). *Acta Cryst.* A**32**, 751–767.

SIMON, A. & PETERS, K. (1980). *Acta Cryst.* B**36**, 2750–2751.

TRÖMEL, M. (1983*a*). *Acta Cryst.* B**39**, 664–669.

TRÖMEL, M. (1983*b*). *Z. Kristallogr.* **162**, 224–226.

TRUTER, M. R., CRUICKSHANK, D. W. J. & JEFFREY, G. A. (1960). *Acta Cryst.* **13**, 855–862.

ZEMANN, J. (1981). *Fortschr. Mineral.* **59**, 95–116.


*Acta Cryst.* (1984). B**40**, 342–346

# Single-Crystal Disorder Diffuse X-ray Scattering from Phase II Ammonium Nitrate, $NH_4NO_3$

BY S. F. WONG, B. E. GILLAN AND B. W. LUCAS*

*Department of Physics, University of Queensland, St Lucia, Brisbane, Queensland* 4067, *Australia*

(*Received* 27 *January* 1984; *accepted* 6 *March* 1984)

**Abstract**

X-ray diffuse scattering from single crystals of phase II (at ~361 K) ammonium nitrate has been recorded on a series of Laue photographs using crystal-monochromatized Cu $K\alpha$ incident radiation. The diffuse scattering due to disordered orientation of the $NO_3$ ions occurs in plate-like shapes perpendicular to the $\mathbf{c}^*$ direction in reciprocal space. The disorder diffuse intensities on the Laue photographs were measured with a scanning microdensitometer and subsequently represented (after various corrections) as equi-intensity contour maps in planar section of reciprocal space. The observed intensity distributions were

* Author to whom correspondence should be addressed.

0108-7681/84/040342-05$01.50

compared with those predicted by extension of a model proposed by Shinnaka [*J. Phys. Soc. Jpn.* (1959), **14**, 1707–1716]. Point-by-point least-squares refinements were used to minimize the difference between calculated and observed intensities. Results show that the model is acceptable to the accuracy (~10%) of the observed intensity data and that correlation exists between nearest-neighbour $NO_3$-ion orientations for the [001] direction, with some small yet significant correlations also along the ⟨110⟩ and ⟨100⟩ directions. Correlations between $NO_3$-ion orientations at greater separation within the (001) planes are negligible.

## Introduction

At atmospheric pressure, $NH_4NO_3$ undergoes the following thermal polymorphic phase transitions (Nagatani, Seiyama, Sakiyama, Suga & Seki, 1967):

$$\begin{aligned} NH_4NO_3(V) &\xrightarrow{255\ K} NH_4NO_3(IV) \\ &\xrightarrow{305{\cdot}3\ K} NH_4NO_3(III) \\ &\xrightarrow{357\ K} NH_4NO_3(II) \\ &\xrightarrow{398\ K} NH_4NO_3(I). \end{aligned}$$

Dry single crystals (without occluded water) have been found to transform directly from phase IV to phase II on heating (at 328 K) and usually retain their single-crystal form through the transition (Brown & McLaren, 1962).

The crystal structures of all five phases have now been determined by neutron diffraction methods (V: Ahtee, Smolander, Lucas & Hewat, 1983; IV: Choi, Mapes & Prince, 1972; III: Lucas, Ahtee & Hewat, 1980; II: Lucas, Ahtee & Hewat, 1979; I: Ahtee, Kurki-Suonio, Lucas & Hewat, 1979).

Shinnaka (1959) has taken single-crystal diffuse X-ray scattering photographs for phase II ammonium nitrate with filtered Cu $K\alpha$ radiation and observed on them some striking patterns of diffuse intensity streaks. These were noted to be more intense than, and additional to, the (normally fairly localized) regions of thermal diffuse scattering. The streaks on the photographs were found to be part of sheets of diffuse scattering distributed about planes of reciprocal space, normal to the $c^*$ axis, and present for $l = \pm 1, \pm 2, \pm 3, \ldots$; the sheet for $l = 0$ was conspicuously absent. From visual estimation of the intensity variation of the diffuse streaks, qualitative intensity contours for the $l = 1, 2, 3$ two-dimensional layers in reciprocal space were produced, over limited regions. Shinnaka (1959) proposed a model with orientational disorder of the $NO_3$ groups, based on the previously published partial Bragg structure determination (Shinnaka, 1956). The theoretically calculated diffuse intensity contours were visually compared with the observed intensity distributions. Although the contour shapes, calculated on the basis of the model, exhibited some features of the observed data contour maps, no quantitative comparison could be made.

In the present work, quantitative measurements of the relative diffuse intensity distribution have been made for comparison with that predicted by an extended version of Shinnaka's (1959) disordered model, and including the more recent Bragg structure details determined by neutron diffraction methods (Lucas *et al.*, 1979). The aim of the present study was to place this comparison on a more quantitative basis.

## Experimental procedures

Single crystals of $NH_4NO_3$(IV) were first grown by slow evaporation of a saturated methanol solution held at a constant temperature of 2 K above room temperature (298 K) over a two week period. The needle-shaped single crystals chosen for the X-ray diffraction study had well defined faces of approximate dimensions $0{\cdot}5 \times 0{\cdot}7 \times 1{\cdot}3$ mm ($NH_4NO_3$ powder of stated minimum purity 99·0% from Ajax Chemicals Ltd, Sydney, was used). Since $NH_4NO_3$ is hygroscopic, sample crystals were sealed in thin-walled glass capillary tubes (marketed by Pantak Ltd, England), with their largest dimension (the $a$ axis) along the tube length. The crystal specimen was mounted on an X-ray diffraction furnace (Lucas, 1973) that was placed on a Unicam oscillation–rotation cylindrical camera of radius 3·0 cm.

Initial photographs were taken at room temperature to check the crystal quality and sample alignment. Since the phase IV→phase II transformation preserves the [100] direction (Brown & McLaren, 1962), the phase II single-crystal sample was obtained by suddenly heating through the transition temperature of 328 K. Laue photographs at 2·5° intervals about the [100] rotation axis, covering a 90° rotation range, were taken at a constant temperature of 361 K, each with half-hour exposure time; care having been taken to remain within the linear range of the film blackening density. All the exposed films were then chemically processed together, under identical conditions. Examples of the photographs obtained are shown in Fig. 1.

The radiation used was monochromatic, achieved by reflecting the incident X-ray beam from the (200) planes of a doubly-curved lithium fluoride single-crystal monochromator, adjusted to give Cu $K\alpha$ radiation.

An automatic recording microdensitometer (Joyce–Loebl Mk IV CS) was used to produce traces of the intensity variation from the photographs. Scans were made on each photograph, with each trace being parallel to the equatorial layer line and increasing

distance from it so that each photograph was effectively scanned. Procedures for the treatment of the scan measurements, including allowance for background intensities, various corrections [including absorption (*International Tables for X-ray Crystallography*, 1968), polarization (Azaroff, 1955), geometrical (Hoerni & Wooster, 1953)] to be applied, interfilm intensity correlation (McMullan, Burns & Ferrier, 1968; Ferrier, McMullan & Sutherland, 1973), and the method (Martin, 1956) for producing corrected equi-diffuse intensity contour maps for the planes in reciprocal space, are all given in detail elsewhere (Wong, 1974).

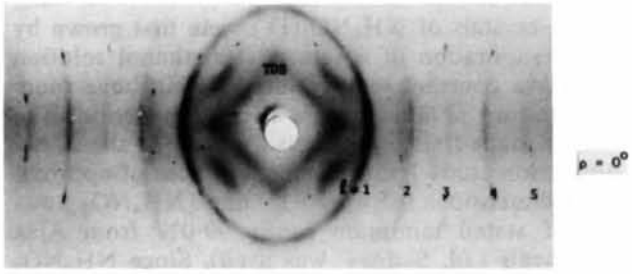


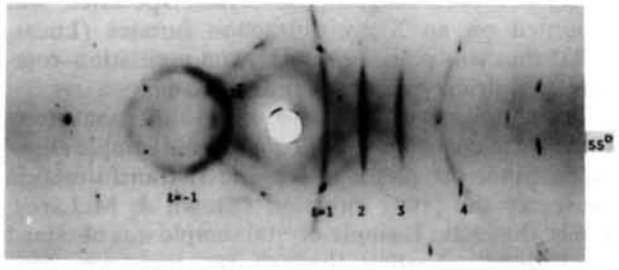


(*b*)

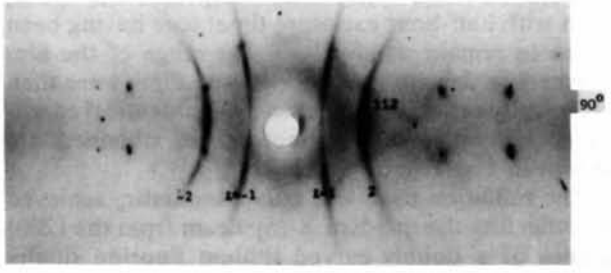


(*c*)

Fig. 1. Representative examples of the series of Laue pattern photographs for tetragonal phase II ammonium nitrate (~361 K) in which the orientations of the ionic groups are disordered. Orientation of the crystal is given by the angle $\rho$, being that between [001] and the direct beam, with [100] vertical. Crystal-monochromatized Cu $K\alpha$ radiation and cylindrical film.

### Shinnaka's (1959) disorder model

Shinnaka (1956) proposed a crystal structure for $NH_4NO_3$(II) with a tetragonal crystal system $a = 5{\cdot}74$, $c = 4{\cdot}95$ Å and $Z = 2$. The $NH_4$ ions were considered to have their nitrogen atoms positioned at (0, 0, $\frac{1}{2}$) and ($\frac{1}{2}$, $\frac{1}{2}$, $\frac{1}{2}$). The $NO_3$ ions were positioned about the points ($\frac{1}{2}$, 0, 0) and (0, $\frac{1}{2}$, 0) and were orientationally disordered, their planes making angles of ±45°, about [001], to the lattice planes (010) and (100), respectively. A more recent neutron diffraction study giving the complete structure has been published (Lucas *et al.*, 1979) and was used in the calculations made for the present study. The H atoms were not, however, included as these would not contribute significantly to the diffuse intensity distribution.

In an attempt to explain the presence of the characteristic diffuse streaks on the X-ray photographs, Shinnaka (1959) proposed a model which considers the probability of orientation of the $NO_3$ group in neighbouring unit cells. He introduced the parameters $\alpha$, $\beta$ such that they represent the probability of nearest-neighbour ions having opposite orientations along the [001] and ⟨110⟩ directions, respectively, and $\gamma$ for the nearest neighbour along the ⟨100⟩ directions. From this he produced an expression to predict the diffuse intensity distribution.

### Least-squares refinements

To allow point-by-point comparison between the observed disorder diffuse scattering and that predicted by Sinnaka's (1959) model the contour maps for the observed data were put into digitized form, by means of a digitizer connected to the University's central computer. Data files were produced for each layer in reciprocal space ($l = 1, 2, 3$). A computer program was written, based on Shinnaka's (1959) model, to minimize the differences (point-by-point) between the observed, $y_i^{obs}$, and calculated, $y_i^{calc}$, disorder diffuse intensity by the least-squares-refinement method. In the refinement, a scale factor(s), $k_j$, and the probability parameters, $\beta$ and $\gamma$, were refined; the parameter $\alpha$ is determined by the 'thickness' of the diffuse planes normal to the $c^*$ axis [according to the Shinnaka (1959) model].

Each plane ($l = 1, 2, 3$) of data was refined separately initially to check that no inconsistencies in the data were apparent, then all the data were refined together to give the best overall fit. The values of the parameters obtained at convergence, together with the residual agreement factor, are given in Table 1. The corresponding calculated contour maps for the three layers ($l = 1, 2, 3$), using the refined parameter values, were overlayed with the corresponding observed contour maps. The general features of the observed and calculated maps agreed, although some quantitative differences were apparent.

Closer agreement between the observed and calculated contour maps was then attempted by introducing the additional nearest-neighbour $NO_3$-ion orientational probability parameters for third-nearest ($\rho$), fourth-nearest ($\sigma$) and fifth-nearest ($\eta$) neighbours in the (001) plane. The expression for the predicted diffuse intensity distribution, incorporating these additional neighbour interactions, is readily obtained (Gillan, 1982) by extension of the Shinnaka (1959) equation:

$$
\begin{aligned}
I_2 = I_e N(&(\overline{|F_1|^2}+\overline{|F_2|^2}-|\bar{F}_1|^2-|\bar{F}_2|^2)\\
&\times\{1+2(1-2\gamma)(\cos 2\pi\mathbf{S}.\mathbf{A}+\cos 2\pi\mathbf{S}.\mathbf{B})\\
&+2(1-2\eta)(\cos 2\pi\mathbf{S}.2\mathbf{A}+\cos 2\pi\mathbf{S}.2\mathbf{B})\\
&+2(1-2\rho)(\cos 2\pi\mathbf{S}.2\mathbf{a}+\cos 2\pi\mathbf{S}.2\mathbf{b})\}\\
&+\{\tfrac{1}{2}[F_1^+(F_2^+)^*+F_1^-(F_2^-)^*+F_2^+(F_1^+)^*\\
&+F_2^-(F_1^-)^*]-\bar{F}_1(\bar{F}_2)^*-\bar{F}_2(\bar{F}_1)^*\}\\
&\times\{2(1-2\beta)(\cos 2\pi\mathbf{S}.\mathbf{a}+\cos 2\pi\mathbf{S}.\mathbf{b})\\
&+2(1-2\sigma)[\cos 2\pi\mathbf{S}.(2\mathbf{a}+\mathbf{b})+\cos 2\pi\mathbf{S}.(2\mathbf{b}+\mathbf{a})\\
&+\cos 2\pi\mathbf{S}.(2\mathbf{a}-\mathbf{b})+\cos 2\pi\mathbf{S}.(\mathbf{a}-2\mathbf{b})]\})J(\mathbf{S}.\mathbf{c}),
\end{aligned}
$$

where the notation is that used by Shinnaka (1959) and the additional symbols defined above. The possibility of larger than anticipated errors being introduced in the inter-film intensity calibration (McMullan *et al.*, 1968; Ferrier *et al.*, 1973) was also considered by allowing refinement with all data points included and individual scale factors ($k_1$, $k_2$, $k_3$) for each plane of data points. The parameter values obtained at convergence of refinement are shown in Table 1. The calculated diffuse intensity contour maps for the latter model are compared with those observed in Fig. 2.

## Discussion

The disorder diffuse intensity distribution has been carefully measured and interlayer intensities correlated. Although the intensities measured are still on a relative scale, it is considered that the intensities are reliable to about 10% and an improvement on the rather limited and visually estimated data of Shinnaka (1959). This more accurate and quantitative observational data allowed, through least-squares refinement procedures, a more reliable test of the Shinnaka (1959) model for ionic disorder in $NH_4NO_3$(II). The values of the $\beta$ and $\gamma$ parameters show small but significant correlation between the relative $NO_3$-ion orientations in the corresponding directions (0·5 would indicate no correlation). The closeness of the $\rho$-, $\sigma$-, $\eta$-parameter values to 0·5, on the other hand, suggests no correlations between orientations for these more distant ions. The significant discrepancies between the individual layer

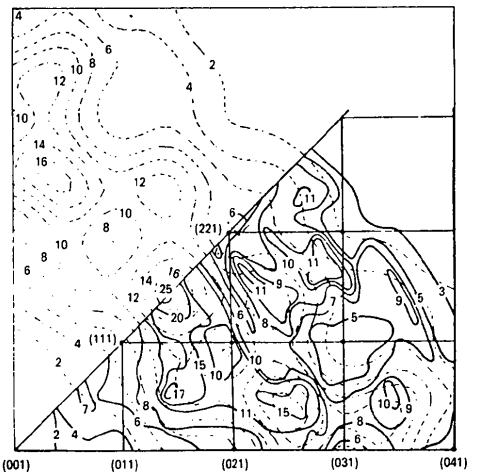


(*a*)

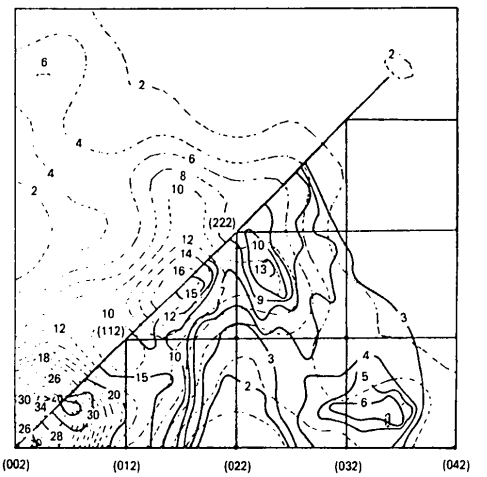


(*b*)

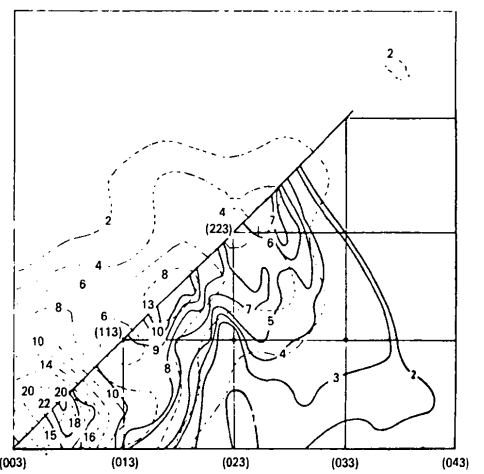


(*c*)

Fig. 2. Disorder diffuse intensity contour maps for the (*a*) first-, (*b*) second- and (*c*) third-order reciprocal-lattice planes. The full-line contours represent the relative observed intensities, while the dashed-line contours are the calculated intensities (scaled to the observed by the least-squares refinement method).

Table 1. *Least-squares refinement results (unit weight, $\omega_i$, assumed)*

| | | Refinement method | | |
|---|---|---|---|---|
| | Shinnaka's (1959) values | Shinnaka's model, one scale factor | Extended model, one scale factor | Extended model, three scale factors |
| Scale factor(s) | | | | 0·143 (3) |
| $k_j$ | — | 0·163 (2) | 0·163 (3) | 0·191 (2) |
| | | | | 0·218 (2) |
| Probability parameters | | | | |
| $\alpha$ | ~0·11 | | 0·131 (13) | |
| $\beta$ | ~0·5 | 0·520 (4) | 0·519 (14) | 0·523 (3) |
| $\gamma$ | ~0·58 | 0·552 (3) | 0·550 (10) | 0·546 (2) |
| $\rho$ | — | — | 0·499 (9) | 0·498 (3) |
| $\sigma$ | — | — | 0·494 (9) | 0·492 (5) |
| $\eta$ | — | — | 0·498 (9) | 0·500 (3) |
| Residual factor | | | | |
| $R=\left[\frac{\sum_i \omega_i(y_i^{obs}-k_j y_i^{calc})^2}{\sum_i \omega_i(y_i^{obs})^2}\right]^{\frac{1}{2}}$ | — | 0·123 | 0·122 | 0·100 |
| $R_{expected}$* | | | 0·104 | |

* $R_{expected}=[(N-P)/\sum_i \omega_i(y_i^{obs})^2]^{1/2}$, where $N$ = number of observed points = 1361, $P$ = number of parameters refined = (3, 6, or 8, depending on model).

scale-factor magnitudes suggest larger errors are introduced during the application of the method used than perhaps would be anticipated.

The final agreement-factor values and contour-map comparison suggest that, while significant discrepancies exist between the observed and calculated diffuse intensity distributions, Shinnaka's (1959) model is acceptable to the accuracy of the presently available observed data.

## References


AHTEE, M., KURKI-SUONIO, K., LUCAS, B. W. & HEWAT, A. W. (1979). *Acta Cryst.* A**35**, 591–598.

AHTEE, M., SMOLANDER, K. J., LUCAS, B. W. & HEWAT, A. W. (1983). *Acta Cryst.* C**39**, 651–655.

AZAROFF, L. V. (1955). *Acta Cryst.* **8**, 701–704.

BROWN, R. N. & MCLAREN, A. C. (1962). *Proc. R. Soc. London Ser. A*, **266**, 329–343.

CHOI, C. S., MAPES, J. E. & PRINCE, E. (1972). *Acta Cryst.* B**28**, 1357–1361.

FERRIER, W. G., MCMULLAN, J. T. & SUTHERLAND, D. C. (1973). *J. Phys. C*, **6**, 1489–1499.

GILLAN, B. E. (1982). *A Theoretical Study of the X-ray Diffuse Scattering by Single-Crystal Phase II Ammonium Nitrate*, BSc (Hons) Report, Univ. of Queensland.

HOERNI, J. & WOOSTER, W. A. (1953). *Acta Cryst.* **6**, 543–547.

*International Tables for X-ray Crystallography* (1968). Vol. III. Birmingham: Kynoch Press.

LUCAS, B. W. (1973). *J. Phys. E*, **6**, 1097–1099.

LUCAS, B. W., AHTEE, M. & HEWAT, A. W. (1979). *Acta Cryst.* B**35**, 1038–1041.

LUCAS, B. W., AHTEE, M. & HEWAT, A. W. (1980). *Acta Cryst.* B**36**, 2005–2008.

MCMULLAN, J. T., BURNS, D. M. & FERRIER, W. G. (1968). *J. Appl. Cryst.* **1**, 293–298.

MARTIN, W. G. (1956). *J. Appl. Phys.* **27**, 514–515.

NAGATANI, M., SEIYAMA, T., SAKIYAMA, M., SUGA, H. & SEKI, S. (1967). *Bull. Chem. Soc. Jpn*, **40**, 1833–1844.

SHINNAKA, Y. (1956). *J. Phys. Soc. Jpn*, **11**, 393–396.

SHINNAKA, Y. (1959). *J. Phys. Soc. Jpn*, **14**, 1707–1716.

WONG, S.-F. (1974). *An X-ray Scattering Study of a Solid-State Phase Transition in Ammonium Nitrate*, MSc Thesis, Univ. of Queensland.